Cold Weather Teleconnections from Future Arctic Sea Ice Loss and Ocean Warming

Y. T. Eunice Lo[1], Daniel M Mitchell[1], Peter A. G. Watson[2], and James A Screen[3]

[1]University of Bristol
[2]School of Geographical Sciences, University of Bristol
[3]University of Exeter

November 21, 2022

Abstract

Rapid Arctic warming and decline in sea ice have been observed in recent decades. These trends will likely continue, potentially changing winter extremes elsewhere in the Northern Hemisphere. We use coordinated Polar Amplification Model Intercomparison Project (PAMIP) experiments to decompose the Northern Hemisphere winter cold temperature responses to future Arctic sea-ice loss and sea surface temperature (SST) change, separately, at 2C global mean warming. Cold extremes (20-year return period) will generally become warmer at high- and mid-latitudes due to Arctic sea-ice loss, with the largest warming in East Canada. SST change will warm cold extremes everywhere, overwhelming simulated sea ice-induced cooling responses in, e.g., southwestern United States. In general, the SST-induced changes dominate over sea ice-induced changes, with exceptions in East Canada, Nunavut (Canada) and North Pacific Russia. Our results suggest that if climate models do not adequately capture the sea-ice and SST components, cold extremes will be biased.

Hosted file

`essoar.10512271.1.docx` available at https://authorea.com/users/518290/articles/597751-cold-weather-teleconnections-from-future-arctic-sea-ice-loss-and-ocean-warming

Hosted file

`submitted_lo_arcticonnect_grl_v4_suppl.docx` available at https://authorea.com/users/518290/articles/597751-cold-weather-teleconnections-from-future-arctic-sea-ice-loss-and-ocean-warming

Y. T. Eunice Lo[1,2], Dann M. Mitchell[1,2], Peter A. G. Watson[1,2], and James A. Screen[3]

[1]School of Geographical Sciences, University of Bristol, Bristol, UK.

[2]Cabot Institute for the Environment, University of Bristol, Bristol, UK.

[3]College of Engineering, Mathematics and Physical Sciences, University of Exeter, Exeter, UK.

Corresponding author: Eunice Lo (eunice.lo@bristol.ac.uk)

Key Points:

- Winter cold extremes in northern mid- and high-latitude land regions will get warmer due to future Arctic sea-ice loss
- Warming due to future sea surface temperature change are larger than that due to sea-ice loss in a majority of the regions
- Even in few places where sea ice causes more severe cold extremes, this effect is overwhelmed by warming due to ocean temperature change

Abstract

Rapid Arctic warming and decline in sea ice have been observed in recent decades. These trends will likely continue, potentially changing winter extremes elsewhere in the Northern Hemisphere. We use coordinated Polar Amplification Model Intercomparison Project (PAMIP) experiments to decompose the Northern Hemisphere winter cold temperature responses to future Arctic sea-ice loss and sea surface temperature (SST) change, separately, at 2°C global mean warming. Cold extremes (20-year return period) will generally become warmer at high- and mid-latitudes due to Arctic sea-ice loss, with the largest warming in East Canada. SST change will warm cold extremes everywhere, overwhelming simulated sea ice-induced cooling responses in, e.g., southwestern United States. In general, the SST-induced changes dominate over sea ice-induced changes, with exceptions in East Canada, Nunavut (Canada) and North Pacific Russia. Our results suggest that if climate models do not adequately capture the sea-ice and SST components, cold extremes will be biased.

Plain Language Summary

Regions near the North Pole have rapidly warmed, and the sea ice has reduced, in recent decades. These will likely continue and change winter cold weather elsewhere in the future. We use climate models that run the same experiments in the Polar Amplification Model Intercomparison Project to study how extremely cold temperatures may change because of Arctic sea-ice loss and ocean warming separately. In a future world that is, on average, 2°C warmer than pre-industrial times, cold extremes will become warmer at high- and mid-latitudes because of sea-ice loss, with the strongest warming in East Canada. Ocean warming will lead to warmer cold extremes everywhere in the Northern Hemisphere. In general, the effect from ocean warming is larger, meaning that even if sea-ice loss

will cause some cooling in some places, this cooling will be overwhelmed by warming by the ocean. This means that climate models need to adequately capture both the sea-ice and ocean temperature components, in order to estimate future cold extremes.

1 Introduction

Polar amplification, the phenomenon where near-surface air temperatures near the poles warm more than the global average in response to external radiative forcing, is a prominent feature of anthropogenic climate change. Since the late 20^{th} century, the Arctic has warmed 3 to 4 times faster than the global mean (Rantanen et al. 2022), and September Arctic sea ice extent has decreased by half (James A. Screen et al. 2018). Arctic amplification is driven by local temperature, surface albedo and cloud feedbacks, and changes in the poleward transport of energy in the atmosphere and ocean (Goosse et al. 2018; Previdi, Smith, and Polvani 2021). It is strongest in boreal winter. Climate models have been shown to be able to reproduce the observed temperature pattern and mean sea ice area in the Arctic, albeit with some discrepancy (Notz and SIMIP Community 2020; Previdi, Smith, and Polvani 2021).

Previous modelling studies have projected a decrease in the likelihood and duration of cold extremes at the high latitudes and over central and eastern North Ameria, but not over central Asia, due to future Arctic sea-ice loss (James A. Screen, Deser, and Sun 2015a, 2015b). Another study has projected no change in the frequency or duration of cold weather outbreaks but a decrease in their severity in the US, Europe and East Asia (Ayarzagüena and Screen 2016).

However, there is uncertainty about the influence of Arctic amplification on atmospheric circulation and mid-latitude severe weather (Cohen et al. 2020). For example, coupled atmosphere-ocean models suggest that Arctic sea-ice loss intensifies the wintertime Siberian High, but the temperature reponse is not robustly simulated (J. A. Screen and Blackport 2019; James A. Screen et al. 2018). Other studies have found contradictory circulation responses (Blackport and Kushner 2016; Nakamura et al. 2015) or causal links (Mori et al. 2019; Zappa, Ceppi, and Shepherd 2021). Different climate models, forcing experiments and methodologies used have contributed to this uncertainty (Overland et al. 2016). This provides a strong reason for using coordinated experiments in a multi-model ensemble.

The Polar Amplification Model Intercomparison Project (PAMIP) is a set of coordinated experiments designed to understand the causes as well as the consequences of polar amplification (Smith et al. 2019). It is a contribution to the Coupled Model Intercomparison Project Phase 6 (CMIP6) (Eyring et al. 2016). By running standardized experiments in different CMIP6 models and generating large ensembles from each model, PAMIP helps to provide a better estimate of the forced response and to quantify model uncertainty (James A. Screen et al. 2018). PAMIP simulations have been used to study, for example, the effects of Arctic sea-ice loss and/or warming on the North Pacific jet stream

(Ronalds et al. 2020), poleward heat transport (Audette et al. 2021), the wintertime Siberian High (Labe, Peings, and Magnusdottir 2020) and mid-latitude westerly winds (Smith et al. 2022).

Here, we utilise PAMIP experiments for the first time to assess the respective responses of boreal winter cold extremes to future Arctic sea-ice loss and sea surface temperature (SST) change associated with 2°C global mean warming above pre-industrial levels. We focus on land regions in the Northern Hemisphere, where extreme cold temperatures have direct impacts on their communities. Using daily minimum temperature output from ten CMIP6 models, each of which having up to 200 ensemble members, we examine the change in 1-in-20-year cold events. Differing from previous studies, we examine the respective responses to sea-ice loss and SST change and highlight that some sea ice-induced local cooling may be overwhelmed by ocean warming.

2 Data and Methods

2.1 PAMIP experiments

We compare mode-simulated temperatures between three PAMIP atmosphere-only time slice experiments. First, we use an experiment forced by present-day (i.e., 1979-2008 climatological) SSTs and sea ice concentration (Smith et al. 2019), denoted as 'pd' hereafter. Second, we use an experiment forced by present-day SSTs but future Arctic sea ice concentration representative of 2°C global average warming above pre-industrial levels. This experiment is denoted as 'futArcSIC'. Third, we make use of an experiment in which climate models are forced by future SSTs representative of 2°C global warming but sea ice concentration at the present-day level. This experiment is referred to as 'futSST' hereafter. We note that 2°C global average warming above pre-industrial levels in these experiments is equivalent to 15.7°C in absolute global mean temperature (Smith et al. 2019), and that there are other methods in defining global warming levels (Uhe et al. 2021). All of these experiments are one-year time slices with radiative forcing from the year 2000. As such, comparing futArcSIC with pd gives us changes due to future Arctic sea-ice loss, whereas comparing futSST with pd gives us changes due to future SST change.

These time-slice experiments are run by CMIP6 models with a minimum of ~100 winters to generate large ensembles that are suitable for studying climate extremes (Smith et al. 2019). We make use of daily minimum near-surface air temperature (tasmin) output from a total of ten CMIP6 models, as listed in Table 1. Specifically, we focus on the respective changes in minimum tasmin in boreal winter (December-January-February, or DJF) due to future Arctic sea ice loss and future SST change. All included models have daily tasmin outputs for pd and futArcSIC. A subset of six models also have outputs for futSST. More than half of the models have at least 200 ensemble members of tasmin simulations at the time this study was carried out. Therefore, we use a maximum of 200 members from each model (Table 1) to compute the differences in 1-in-20-year winter minimum temperature at grid scale due to Arctic sea-ice

loss and SST change, respectively. We use the 20-year return period to represent cold extremes. We conduct an additional return period analysis at the regional scale (Sections 2.2 and 2.3), focusing on the 2-year and 20-year return periods.

Table 1. The CMIP6 models used in this study.

Model	Experiments (ensemble sizes)	Reference
AWI-CM-1-1-MR	pd (100), futArcSIC (100), futSST (100)	(Semmler et al. 2020)
CanESM5	pd (200), futArcSIC (200), futSST (100)	(Swart et al. 2019)
CESM2	pd (200), futArcSIC (100), futSST (200)	(Danabasoglu et al. 2020)
CNRM-CM6-1	pd (200), futArcSIC (200)	(Voldoire et al. 2019)
FGOALS-f3-L	pd (100), futArcSIC (100), futSST (100)	(He et al. 2019)
HadGEM3-GC31-MM	pd (200), futArcSIC (200), futSST (200)	(Andrews et al. 2020)
IPSL-CM6A-LR	pd (200), futArcSIC (200), futSST (200)	(Boucher et al. 2020)
MIROC6	pd (100), futArcSIC (100)	(Tatebe et al. 2019)
NorESM2-LM	pd (200), futArcSIC (200)	(Seland et al. 2020)
TaiESM1	Pd (95), futArcSIC (69)	(Wang et al. 2021)

The included CMIP6 models have different atmospheric horizontal resolutions, ranging from 0.83° x 0.56° in HadGEM3-GC31-MM (Andrews et al. 2020) to ~2.8° in CanESM5 (Swart et al. 2019). For all grid cells in the Northern Hemisphere, we calculate the difference in 1-in-20-year minimum temperature between the PAMIP experiments in individual models, as well as the multi-model mean difference (giving each model equal weight). When considering the individual models, we compute the temperature difference in the models' native grids. When considering the multi-model mean, we regrid all model results to CanESM5's grid because it is the coarsest among the studied models, before computing the multi-model mean difference.

2.2 Regions

We perform analyses in 14 selected regions in the northern mid to high latitudes. These regions are selected from a pre-defined set of regions that are ~2 Mm^2 in size and designed for examining climate extremes and their impacts (Stone 2019). The included regions are: Alaska, NWT and Yukon, West Canada, Nunavut, Manitoba and Ontario, East Canada, Greenland, North EEA, Northwest Russia, Southwest Russia,West Siberia, Northeast Siberia, Sakha, and North Pacific Russia (Figure S1).

2.3 Return period analysis

We compute return periods by sorting each temperature series of DJF minimum tasmin in ascending order and dividing the length of the series by the ranks of the temperature values within the sorted series. We find the difference in 1-in-20-year temperature between experiments at grid scale. We test whether the two samples of minimum temperature from two different experiments are significantly different using a Kolmogorov-Smirnov (KS) test (Daniel 1990).

For the regional analysis, we produce and compare return period curves from the pd simulations and the ERA5 reanalysis (Hersbach et al. 2020). We find the regional mean DJF minimum tasmin by area-weighted averaging values across native grid cells whose grid point values are within the boundary of each region. Since the present-day conditions in pd are based on 1979-2008 climatology, we extract ERA5 data from the same time period for comparison. This comparison is not completely like-for-like because inter-annual variability exists in ERA5 but not in pd, which has constant boundary forcing. To remove the climate change signal from the regional ERA5 time series and approximately isolate internal variability, we fit a linear trend to the corresponding DJF mean tasmin time series and remove this trend from the DJF minimum tasmin time series. This ensures that the trend in the winter season, not just in the extremes, is removed. We then add the regional 1995-2005 average DJF minimum tasmin value in ERA5 to the detrended data, to obtain absolute temperatures for comparison with model output . We choose the 1995-2005 decade because it is centred on year 2000, the year from which radiative forcing is used in the PAMIP time slice experiments.

The modelled pd data do not need detrending because they come from large ensembles of time slice simulations. To bias-correct data from each model, we remove from each ensemble member the bias between ensemble-mean regional-mean DJF minimum tasmin and the 1979-2008 mean regional-mean ERA5 value. We then find the return period curves based on bias-corrected pd data and detrended ERA5 data, respectively.

We estimate the uncertainty associated with the ERA5 return period curve by resampling the ERA5 distribution 1000 times, though acknowledging that uncertainty sampling in the extremes is limited by the observations. This comparison between individual model return period curves and the ERA5 90% confidence interval enables us to identify models that simulate DJF minimum tasmin in present-day climate reasonably well in the selected regions. The left panel of Figure 1 shows this comparison for North EEA, for which four models (CESM2, CNRM-CM6-1, MIROC6 and NorESM2-LM) are excluded in model selection because their return period curves are outside the ERA5 envelope at multiple return time points.

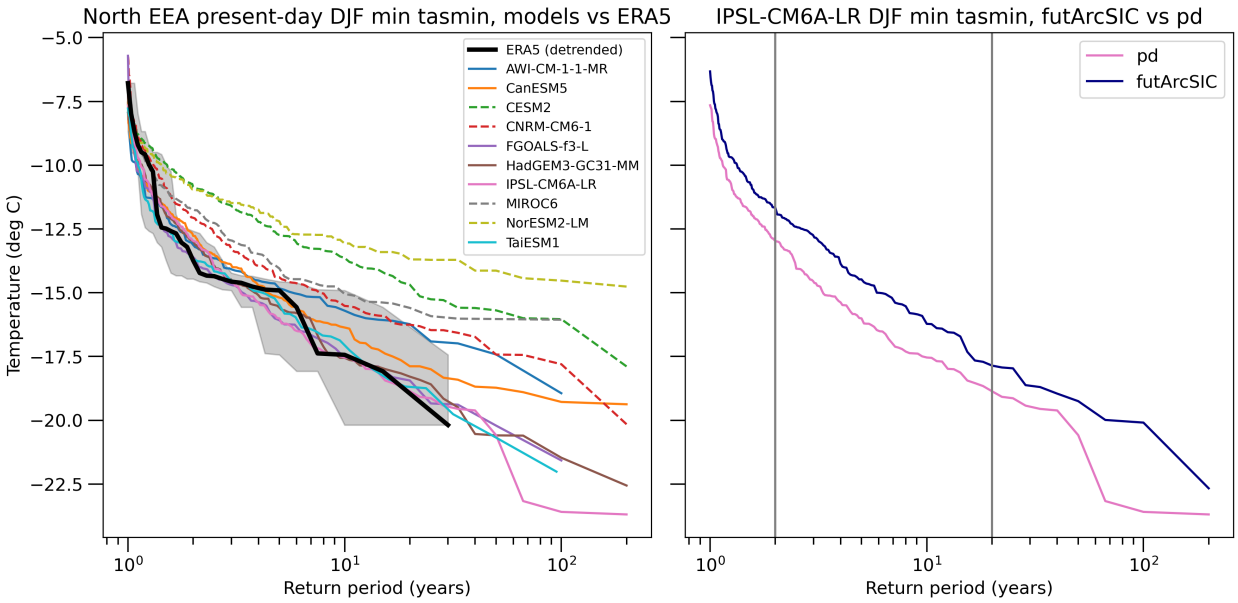

Figure 1. DJF minimum daily minimum temperature return period curves for North EEA. The left panel shows the comparison between present-day bias-corrected data from individual climate models (colored lines) and detrended ERA5 over the period 1979-2008 (thick black line). The grey envelope shows the 90% uncertanty associated with the ERA5 curve found by bootstrapping. Solid colored lines indicate models that are included because they largely fall within the ERA5 envelope, whereas dashed colored lines indicate excluded models. The right panel shows results from the IPSL-CM6A-LR model, for the pd (pink line) and futArcSIC (navy line) experiments. The grey vertical lines indicate the 2-year and 20-year return periods.

To assess the effects of future Arctic sea-ice loss and SST change on regional DJF minimum temperatures, we find the return period curves using the futArcSIC and futSST ensembles, respectively. Example return period curves from futArcSIC and pd simulated by IPSL-CM6A-LR for the North EEA region are shown in the right panel of Figure 1. For each model and region, we find the temperature difference between futArcSIC and pd, and between futSST and pd, at the 2-year and 20-year return periods. For the analysis involving futArcSIC, we report the temperature differences from the individual models, as well as the multi-model mean across all 10 models and the mean across a subset of models that simulate the present day well (according to ERA5). This subset varies from region to region (Figure S2). For the analysis involving futSST, we mainly report the multi-model mean temperature difference across the 6 models for which there is output for this experiment (Table 1), due to a limited number of available models.

3 Results

3.1 Reponse to sea-ice loss

Figure 2 shows the difference in 1-in-20-year winter minimum temperature between futArcSIC and pd in the Northern Hemisphere at grid scale: the multi-model mean and results from individual climate models. All models show the largest warming, of over ~2.5°C, in northern and eastern Canada near Hudson Bay. This is statistically significant at the 5% level and indicates amplified warming in boreal winter minimum temperature due solely to future Arctic sea-ice loss, as future global average temperature is 1.4°C higher in futArcSIC than in pd (Smith et al. 2019). Also generally consistent across the models is ~2°C warming in Alaska. These results are consistent with the imposed sea ice reductions in Hudson Bay, Labrador Sea and Bering-Chukchi Seas in the boreal winter season (Smith et al. 2022).

In the multi-model mean, ~1°C warming is simulated in Greenland, across Scandanavia and in northern Russia. However, there is inconsistency in the sign between the models, with MIROC6 and TaiESM1 simulating some cooling in central Greenland, CanESM5 and CESM2 simulating cooling over Scandanavia, and four models (CESM2, FGOALS-f3-L, MIROC6 and NorESM2-LM) simulating cooling in different parts of north Russia.

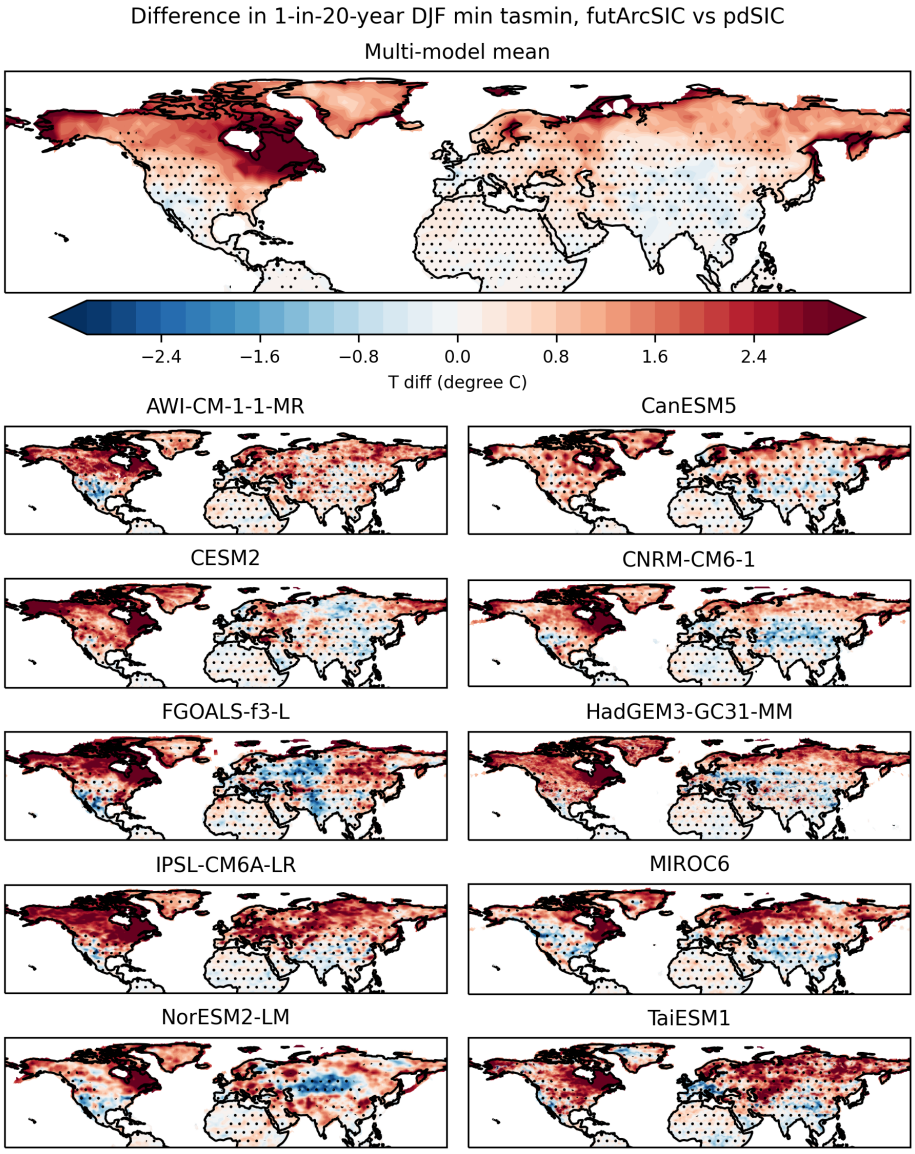

Figure 2. Changes in 1-in-20-year DJF minimum of daily minimum temperature in the Northern Hemisphere due to future Arctic sea-ice loss. The top panel shows the multi-model mean across ten CMIP6 models, whereas the other panels show the results from the individual models. Stippling indicates where results are not statistically significant at the 5% level, based on a KS test.

At the mid and low latitudes, cooling responses are simulated for the United States, parts of Europe and central and eastern Asia. In some models, this cooling is up to about -1°C, suggesting intensified winter cold extremes. However,

this response is not statistically significant at the 5% level and is less robust in terms of spatial extent and magnitude than the aforementioned higher-latitude warming response.

With larger and statistically significant temperature responses to future Arctic sea-ice loss simulated at higher latitudes, we examine the difference in DJF minimum tasmin between futArcSIC and pd at the 2-year and 20-year return periods in 14 selected regions. Figure 3 shows the results from the individual models (circles), as well as the multi-model mean difference across the 10 models (yellow cross) and the multi-model mean difference across selected models that simulate regional present-day climates that are consistent with the ERA5 reanalysis (black square). A filled circle indicates inclusion of the corresponding model in this selected model mean, whereas an empty circle indicates exclusion.

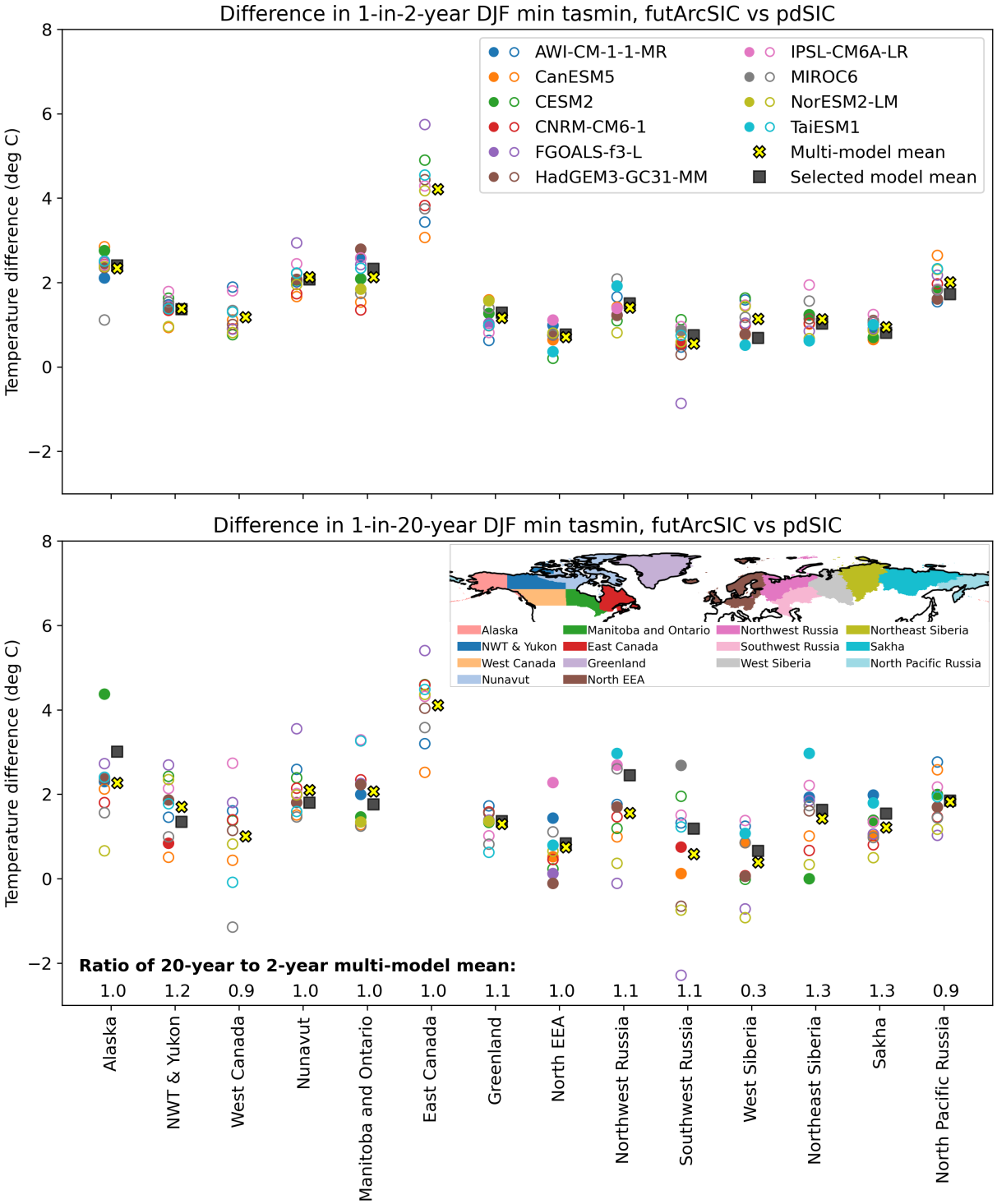
Difference in 1-in-2-year DJF min tasmin, futArcSIC vs pdSIC
Temperature difference (deg C)
AWI-CM-1-1-MR
CanESM5
CESM2
CNRM-CM6-1
FGOALS-f3-L
HadGEM3-GC31-MM
IPSL-CM6A-LR
MIROC6
NorESM2-LM
TaiESM1
Multi-model mean
Selected model mean
Difference in 1-in-20-year DJF min tasmin, futArcSIC vs pdSIC
Temperature difference (deg C)
Alaska
NWT & Yukon
West Canada
Nunavut
Manitoba and Ontario
East Canada
Greenland
North EEA
Northwest Russia
Southwest Russia
West Siberia
Northeast Siberia
Sakha
North Pacific Russia
Ratio of 20-year to 2-year multi-model mean:
1.0 1.2 0.9 1.0 1.0 1.0 1.1 1.0 1.1 1.1 0.3 1.3 1.3 0.9

Figure 3. Top panel: temperature difference in DJF minimum daily minimum temperature with a 2-year return period between futArcSIC and pd, in 14 chosen regions (locations of which are shown in the inset). Each circle represents one CMIP6 model, with a filled circle indicating consistency between that model's bias-corrected pd return period curve and the equivalent ERA5 return period curve from 1979-2008 for the region. Black squares show the mean across the selected models indicated by the filled circles. Yellow crosses show the mean across all ten models. Bottom panel: same as top panel but at a 20-year return period. The numbers above the bottom x-axis indicate the ratios of the 1-in-20-year multi-model mean response to the corresponding 1-in-2-year multi-model mean response.

Like in Figure 2, the regional analysis reveals the largest average warming response in East Canada, with the models simulating regional mean warming between 2 and 6°C at both return periods. In this region and West Canada, no model generates a present-day return period curve that is consistent with that of detrended ERA5, even after mean bias correction. Among the included models, HadGEM3-GC31-MM shows present-day boreal winter minimum temperature consistency with ERA5 in the highest number of regions (8 out of 14; Figure S2).

In the multi-model mean difference of the 1-in-2 year temperature (top panel of Figure 3), all selected regions are projected to experience warming ranging from 0.6°C (inter-model range: to -0.9 to 1.1°C) in Southwest Russia to 4.2°C (range: 3.1 to 5.7°C) in East Canada. The mean results are similar across the subsets of models that simulate regional present-day temperatures that are consistent with ERA5's. Only one model in one region simulates a cooling response: FGOALS-f3-L in Southwest Russia. Modelling uncertainty in the sign and mechanisms of the temperature response in this region due to Arctic sea-ice loss has been documented in the literature (Smith et al. 2022; Zappa, Ceppi, and Shepherd 2021).

At the 20-year return period, the multi-model mean responses are also positive across all regions (bottom panel of Figure 3), with values ranging from 0.4°C (range: -0.9 to 1.4°C) in West Siberia to 4.1°C (range: 2.5 to 5.4°C) in East Canada. More models simulate a cooling response in more regions at the 20-year return period than the 2-year period, including in West Canada, North EEA, Northwest and Southwest Russia, and West and Northeast Siberia.

Comparing the multi-model mean responses between the two return periods (ratios of the 1-in-20-year value to the 1-in-2-year value are shown at the bottom of Figure 3), the 1-in-20-year extremes are projected to warm as much as or more than 1-in-2-year cold weather in 11 of the studied regions. The exceptions are West Canada, West Siberia and North Pacific Russia.

3.2 Repsonse to SST change

The top panel of Figure 4 shows that warmer SSTs associated with 2°C global mean warming increase 1-in-20-year cold temepratures over land in the Northern

Hemisphere in the multi-model mean. This warming is statistically significant at the 5% level. No cooling response is shown in the multi-model mean.

In general, individual models agree on a strong (~3°C) warming signal in North America, particularly in the western parts (Figure S3). The temperature response in Eurasia to future SST change is more variable, with IPSL-CM6A-LR showing strong warming in the northern parts, whereas FGOALS-f3-L showing cooling in those parts but relatively strong warming in east Asia. Regional-mean temperature responses (in the 14 selected regions) to future SST change at the 2- and 20-year return periods are shown in Figure S4.

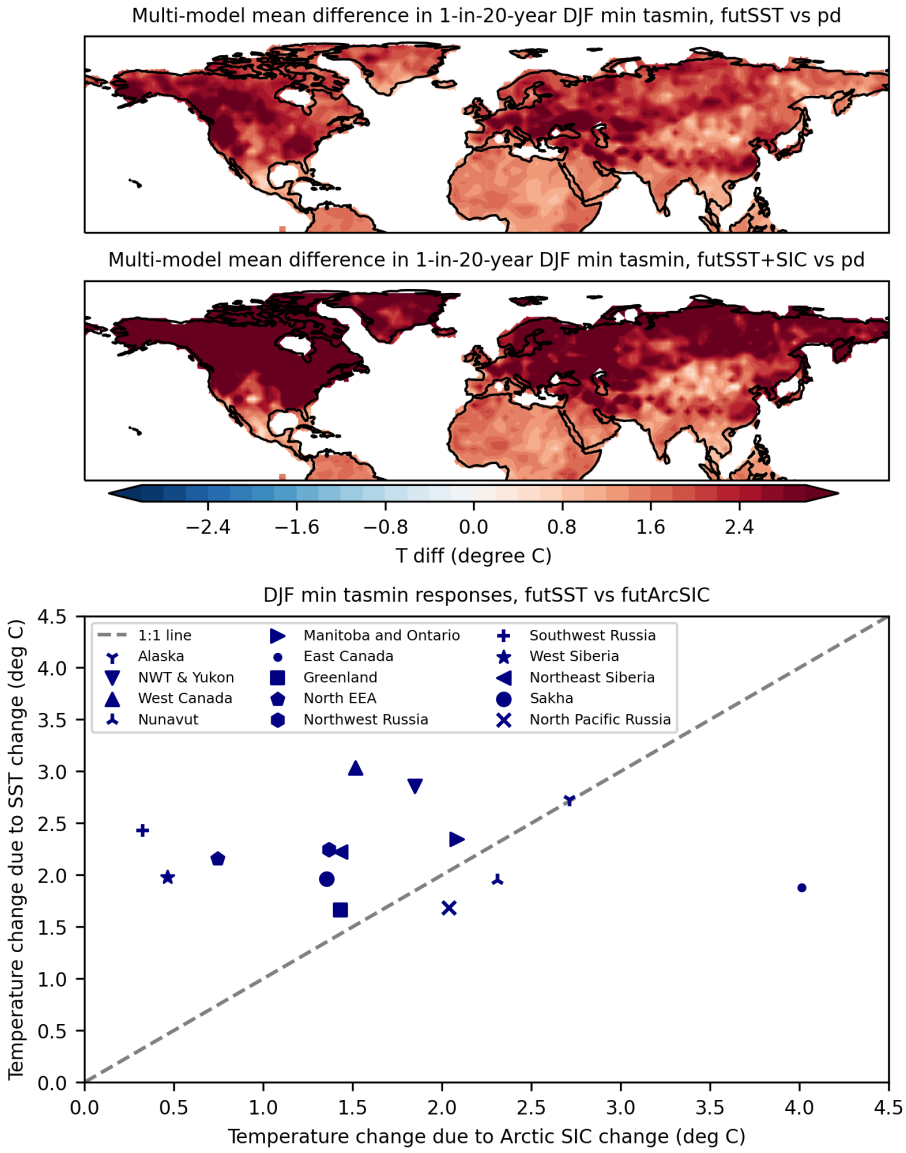

Figure 4. Top panel: multi-model mean changes in 1-in-20-year DJF minimum of daily minimum temperature in the Northern Hemisphere due to future SST change. All changes are statistically significant at the 5% level based on a KS test. Middle panel: the combined response in the multi-model mean to both future SST and sea-ice changes. Bottom panel: comparison between the multi-model mean temperature change in 1-in-20-year minimum DJF daily minimum temperature due to future Arctic sea-ice loss (x-axis) and the corresponding change due to future SST change (y-axis). Each point represents the regional

mean in one particular region. The dashed line indicates a 1:1 relationship.

With previous evidence that responses to sea ice and greenhouse gas forcing are linearly additive (McCusker et al. 2017), it may be reasonable to deduce the combined mean 1-in-20-year minimum temperature response to Arctic sea-ice loss and ocean warming from the top panels of Figures 2 and 4. This is shown in the middle panel of Figure 4. Even in places where Arctic sea-ice loss is simulated to intensify cold extremes (e.g., in southwestern United States, parts of Europe, central and eastern Asia, though not statistically significantly), warming due to SST change overwhelms this cooling effect, resulting in net warming.

We further compare the multi-model mean of the 1-in-20-year temperature difference due to Arctic sea-ice change (x-axis) and SST change (y-axis) over the 14 selected regions in the bottom panel of Figure 4. Only the six models that have daily tasmin output for futSST (Table 1) are included here, regardless of whether their pd counterparts are consistent with detrended 1979-2008 ERA5 data. This is partly due to the limited number of models and partly based on the finding that the multi-model mean and the mean across subsets of models give similar results (Figure S4).

In 11 of the regions (i.e., except for Nunavut, East Canada and North Pacific Russia), the multi-model mean warming response to future SST change is larger than or equal to the response to future Arctic sea-ice loss. The ratio of SST change-induced response to sea ice loss-induced response ranges from 0.5 in East Canada and 0.8 in Nunavut and North Pacific Russia, to 4.3 in West Siberia and 7.5 in Southwest Russia. This demonstrates different respective contributions of future SST change and Arctic sea-ice loss to winter cold extreme changes across the selected regions. Since all selected regions are projected to experience multi-model mean warming to both sea-ice and SST changes, an enhanced combined response is expected. For East Canada, this may mean a combined response of 5.8°C.

5 Discussion and Conclusions

Arctic amplification has been a topic of interest in the literature, not only because it is one of the strongest anthropogenic climate change signals, but also because of its effects on the climate system (Labe, Peings, and Magnusdottir 2020; James A. Screen et al. 2013). This study is the first to use targeted and coordinated PAMIP experiments to decompose the 1-in-20-year winter cold extreme changes associated with Arctic sea-ice loss and SST change in the Northern Hemisphere mid and high latitudes, at 2°C global mean warming above pre-industrial levels. It is also the first to bias-correct the PAMIP simulations and apply model selection based on reanalysis data.

We have shown a multi-model mean warming response to future Arctic sea-ice loss for all selected regions in the mid and high latitudes. This is consistent with the projected decrease in the likelihood and severity of mid- and high-latitude cold extremes in previous studies. For 9 of the 14 selected regions (excluding

West Canada, North EEA, Northwest and Southwest Russia and West Siberia), there is robustness in the sign of change in winter cold extremes across ten CMIP6 models. Where a cooling response is simulated in some models, these results may be sensitive to sampling (not shown), although our Eurasia results are consistent with previous reseach about Arctic warming and Eurasian (Zappa, Ceppi, and Shepherd 2021) and Siberian cooling in boreal winter (Labe, Peings, and Magnusdottir 2020).

The winter cold extreme response to future SST change is more robust, with almost all of the Northern Hemisphere showing a warming response in all available models. Notably, this warming response exceeds the sea ice-induced cooling response in southwestern United States, western Europe and central and eastern Asia, highlighting the importance of comparing the magnitude of the response to sea-ice loss to that to SST change. In the multi-model mean, the SST-induced response is stronger that the sea ice-induced response in 11 of the 14 selected northern regions. Sea-ice loss does not happen in isolation, but considering it together with future ocean warming is not routinely done in the literature. Going forward, researchers should place a stronger focus on the SST component or the net response.

Overall, our results imply that some adverse impacts of cold extremes on, for instance, human health (Mäkinen 2007; Vasconcelos et al. 2013) and transport and power supply (James A. Screen, Deser, and Sun 2015b) are expected to be lessened in the mid and high latitudes in the future. However, we stress that Arctic warming and sea-ice loss are already impacting the Arctic communities (Moerlein and Carothers 2012), whose lifestyles and livelihoods were adapted to cold weather through generations of lived knowledge. Moreover, the combined effect of Arctic sea-ice loss, SST change, and multiple other forcings on winter cold extremes has not been studied here. Future work is important to quantify this and the resulting impacts on various aspects of society through coupled climate and impact modelling.

Impacts are not limited to a change in winter cold extremes. Increasingly for the Arctic region, mild winter conditions are becoming a concern because rain on snow events have wide-ranging impacts on vegetation, soil organisms, Arctic species and human livelihoods (Serreze et al. 2021). Future work should also investigate changes in Arctic winter warm extremes due to future sea-ice loss and SST change.

Acknowledgments

We thank Tim Woollings for providing feedback to this manuscript. This work was funded by the NERC grant ArctiCONNECT (grant ID: NE/V005855/1). PAGW was supported by ArctiCONNECT and a NERC Independent Research Fellowship (grant no. NE/S014713/1). The authors have no conflicts of interests.

Availability Statement

The PAMIP data used in this study are available at Earth System Grid Federation (ESGF) via https://esgf-node.llnl.gov/search/cmip6/. A user guide for creating an ESGF account and downloading the data can be found at https://esgf.github.io/esgf-user-support/. PAMIP data information from each modeling center, including their contact information, can be found at https://www.cesm.ucar.edu/projects/CMIP6/PAMIP/.

References

Andrews, Martin B. et al. 2020. "Historical Simulations With HadGEM3-GC3.1 for CMIP6." *Journal of Advances in Modeling Earth Systems* 12(6): 1–34.Audette, Alexandre et al. 2021. "Opposite Responses of the Dry and Moist Eddy Heat Transport Into the Arctic in the PAMIP Experiments." *Geophysical Research Letters* 48(9): 1–10.Ayarzagüena, Blanca, and James A. Screen. 2016. "Future Arctic Sea Ice Loss Reduces Severity of Cold Air Outbreaks in Midlatitudes." *Geophysical Research Letters* 43(6): 2801–9.Blackport, Russell, and Paul J. Kushner. 2016. "The Transient and Equilibrium Climate Response to Rapid Summertime Sea Ice Loss in CCSM4." *Journal of Climate* 29(2): 401–17.Boucher, Olivier et al. 2020. "Presentation and Evaluation of the IPSL-CM6A-LR Climate Model." *Journal of Advances in Modeling Earth Systems* 12(7): 1–52.Cohen, J. et al. 2020. "Divergent Consensuses on Arctic Amplification Influence on Midlatitude Severe Winter Weather." *Nature Climate Change* 10(1): 20–29.Danabasoglu, G. et al. 2020. "The Community Earth System Model Version 2 (CESM2)." *Journal of Advances in Modeling Earth Systems* 12(2): 1–35.Daniel, Wayne W. 1990. *Applied Nonparametric Statistics*. 2nd ed. PWS-KENT Pub.Eyring, Veronika et al. 2016. "Overview of the Coupled Model Intercomparison Project Phase 6 (CMIP6) Experimental Design and Organization." *Geoscientific Model Development* 9(5): 1937–58.Goosse, Hugues et al. 2018. "Quantifying Climate Feedbacks in Polar Regions." *Nature Communications* 9(1). http://dx.doi.org/10.1038/s41467-018-04173-0.He, Bian et al. 2019. "CAS FGOALS-F3-L Model Datasets for CMIP6 Historical Atmospheric Model Intercomparison Project Simulation." *Advances in Atmospheric Sciences* 36(8): 771–78.Hersbach, Hans et al. 2020. "The ERA5 Global Reanalysis." *Quarterly Journal of the Royal Meteorological Society* (March): 1–51.Labe, Zachary, Yannick Peings, and Gudrun Magnusdottir. 2020. "Warm Arctic, Cold Siberia Pattern: Role of Full Arctic Amplification Versus Sea Ice Loss Alone." *Geophysical Research Letters* 47(17): 1–11.Mäkinen, Tiina M. 2007. "Human Cold Exposure, Adaptation, and Performance in High Latitude Environments." *American Journal of Human Biology* 19(2): 155–64.McCusker, K. E. et al. 2017. "Remarkable Separability of Circulation Response to Arctic Sea Ice Loss and Greenhouse Gas Forcing." *Geophysical Research Letters* 44(15): 7955–64.Moerlein, Katie J., and Courtney Carothers. 2012. "Total Environment of Change: Impacts of Climate Change and Social Transitions on Subsistence Fisheries in Northwest Alaska." *Ecology and Society* 17(1).Mori, Masato et al. 2019. "A Reconciled Estimate of the Influence of Arctic Sea-Ice Loss on Recent Eurasian Cooling." *Nature Climate Change* 9(2): 123–29. http://dx.doi.org/10.1038/s41558-018-0379-3.Nakamura, Tetsu et al. 2015. "A

Negative Phase Shift of the Winter AO/NAO Due to the Recent Arctic Sea-Ice Reduction in Late Autumn." *Journal of Geophysical Research: Atmospheres* 120: 3209–27.Notz, Dirk, and SIMIP Community. 2020. "Arctic Sea Ice in CMIP6." *Geophysical Research Letters* 47(10): 1–11.Overland, James E. et al. 2016. "Nonlinear Response of Mid-Latitude Weather to the Changing Arctic." *Nature Climate Change* 6(11): 992–99.Previdi, Michael, Karen L Smith, and Lorenzo M Polvani. 2021. "Arctic Amplification of Climate Change: A Review of Underlying Mechanisms." *Environmental Research Letters* 16(9): 093003.Rantanen, Mika et al. 2022. "The Arctic Has Warmed Nearly Four Times Faster than the Globe since 1979." *Communications Earth & Environment* 3(168): 1–10.Ronalds, Bryn et al. 2020. "North Pacific Zonal Wind Response to Sea Ice Loss in the Polar Amplification Model Intercomparison Project and Its Downstream Implications." *Climate Dynamics* 55(7–8): 1779–92. https://doi.org/10.1007/s00382-020-05352-w.Screen, J. A., and R. Blackport. 2019. "How Robust Is the Atmospheric Response to Projected Arctic Sea Ice Loss Across Climate Models?" *Geophysical Research Letters* 46(20): 11406–15.Screen, James A. et al. 2018. "Consistency and Discrepancy in the Atmospheric Response to Arctic Sea-Ice Loss across Climate Models." *Nature Geoscience* 11(3): 155–63. http://dx.doi.org/10.1038/s41561-018-0059-y.Screen, James A., Clara Deser, and Lantao Sun. 2015a. "Projected Changes in Regional Climate Extremes Arising from Arctic Sea Ice Loss." *Environmental Research Letters* 10(8).———. 2015b. "Reduced Risk of North American Cold Extremes Due to Continued Arctic Sea Ice Loss." *Bulletin of the American Meteorological Society* 96(9): 1489–1503.Screen, James A., Ian Simmonds, Clara Deser, and Robert Tomas. 2013. "The Atmospheric Response to Three Decades of Observed Arctic Sea Ice Loss." *Journal of Climate* 26(4): 1230–48.Seland, Øyvind et al. 2020. "The Norwegian Earth System Model, NorESM2 – Evaluation of TheCMIP6 DECK and Historical Simulations." *Geoscientific Model Development Discussions* (February): 1–68.Semmler, Tido et al. 2020. "Simulations for CMIP6 With the AWI Climate Model AWI-CM-1-1." *Journal of Advances in Modeling Earth Systems* 12(9): 1–34.Serreze, Mark C. et al. 2021. "Arctic Rain on Snow Events: Bridging Observations to Understand Environmental and Livelihood Impacts." *Environmental Research Letters* 16(10).Smith, D. M. et al. 2019. "The Polar Amplification Model Intercomparison Project (PAMIP) Contribution to CMIP6: Investigating the Causes and Consequences of Polar Amplification." *Geoscientific Model Development Discussions* 12: 1139–64.———. 2022. "Robust but Weak Winter Atmospheric Circulation Response to Future Arctic Sea Ice Loss." *Nature Communications* 13(1): 1–15.Stone, Dáithí A. 2019. "A Hierarchical Collection of Political/Economic Regions for Analysis of Climate Extremes." *Climatic Change* 155(4): 639–56.Swart, Neil C. et al. 2019. "The Canadian Earth System Model Version 5 (CanESM5.0.3)." *Geoscientific Model Development* 12(11): 4823–73.Tatebe, Hiroaki et al. 2019. "Description and Basic Evaluation of Simulated Mean State, Internal Variability, and Climate Sensitivity in MIROC6." *Geoscientific Model Development* 12(7): 2727–65.Uhe, Peter et al. 2021. "Method Uncertainty Is Essential for Reliable Confidence Statements of Precipitation Projections." *Journal of Climate* 34(3):

1227–40.Vasconcelos, João et al. 2013. "The Impact of Winter Cold Weather on Acute Myocardial Infarctions in Portugal." *Environmental Pollution* 183: 14–18. http://dx.doi.org/10.1016/j.envpol.2013.01.037.Voldoire, A. et al. 2019. "Evaluation of CMIP6 DECK Experiments With CNRM-CM6-1." *Journal of Advances in Modeling Earth Systems*.Wang, Yi Chi et al. 2021. "Performance of the Taiwan Earth System Model in Simulating Climate Variability Compared With Observations and CMIP6 Model Simulations." *Journal of Advances in Modeling Earth Systems* 13(7): 1–28.Zappa, Giuseppe, Paulo Ceppi, and Theodore G. Shepherd. 2021. "Eurasian Cooling in Response to Arctic Sea-Ice Loss Is Not Proved by Maximum Covariance Analysis." *Nature Climate Change* 11(2): 106–8. http://dx.doi.org/10.1038/s41558-020-00982-8.